Physics Letters B 754 (2016) 6–10

Contents lists available at ScienceDirect

Physics Letters B

www.elsevier.com/locate/physletb

Production of multistrange hadrons, light nuclei and hypertriton in central Au+Au collisions at $\sqrt{s_{NN}} = 11.5$ and 200 GeV

N. Shah *, Y.G. Ma, J.H. Chen, S. Zhang

Shanghai Institute of Applied Physics, Chinese Academy of Sciences, Shanghai 201800, China

ARTICLE INFO

Article history:
Received 17 November 2015
Received in revised form 6 January 2016
Accepted 6 January 2016
Available online 8 January 2016
Editor: W. Haxton

Keywords:
Strangeness
Nuclei
Hypertriton
Dibaryon

ABSTRACT

The production of dibaryons, light nuclei and hypertriton in the most central Au+Au collisions at $\sqrt{s_{NN}} = 11.5$ and 200 GeV is investigated by using a naive coalescence model. The production of light nuclei is studied and found that the production rate reduces by a factor of 330 (1200) for each extra nucleon added to nuclei at $\sqrt{s_{NN}} = 11.5$ (200) GeV. The p_T integrated yield of multistrange hadrons falls exponentially as strangeness quantum number increases. We further investigate strangeness population factors S_3, S_2 as a function of transverse momentum as well as $\sqrt{s_{NN}}$. The calculations for $\sqrt{s_{NN}} = 11.5$ GeV presented here will stimulate interest to carry out these measurements during the phase-II of beam energy scan program at STAR experiment.

1. Introduction

The experiments at Relativistic Heavy Ion Collider (RHIC) have shown evidence for the hot and dense matter, also known as quark gluon plasma (QGP), created during the early stages of the collisions [1–4]. The high temperature and baryon density of the produced matter make it most suitable environment for the production of light nuclei (p, d, ^{3}He, ^{4}He), hypertriton and dibaryons ($\Lambda\Lambda$, pΩ, $\Xi\Xi$, $\Omega\Omega$) as well as their antiparticles.

For long time the study of light (anti)nuclei and (anti)hypernuclei production has remained of interest to physicists [5,6]. These studies are important to understand the matter–antimatter symmetry, dark matter and structure of neutron star [7,8]. Antihypertriton ($^3_{\bar{\Lambda}}\bar{\mathrm{H}}$) and antihelium-4 ($^4\bar{\mathrm{He}}$) have already been observed at RHIC [9,10] and Large Hadron Collider [11]. Very recently, interaction between antiproton pairs has been also measured by the STAR experiment [12]. The production of light (anti)nuclei and (anti)hypernuclei in heavy ion collisions is fairly described by the thermal model [13,14] and the coalescence model based on multiphase transport model as well as other transport models [15–18]. The production of light (anti)nuclei and (anti)hypernuclei in the most central Au+Au collisions at $\sqrt{s_{NN}} = 200$ GeV has been studied using coalescence model and hydrodynamic blast-wave model in [19,20]. Using the same model of Ref. [19], the production of light (anti)nuclei and (anti)hypernuclei in the most central Au+Au collisions at $\sqrt{s_{NN}} = 11.5$ GeV is discussed in this article.

Different quantum chromodynamics (QCD) based models have proposed existence of dibaryons as exotic form of matter. The H dibaryon was first predicted by Jaffe [21] and then later many other dibaryon states were predicted, e.g. pΩ [22], $\Xi\Xi$ [23] and $\Omega\Omega$ [24]. Recently experiments at RHIC [25] and LHC [26] have searched for H dibaryon. With the advancement in computation power reasonable theoretical progress has been made to understand dibaryon structure [27–31]. However information about the invariant yield of dibaryons from heavy ion collisions remains scarce and more efforts are required in this direction. The invariant yields of dibaryons $\Lambda\Lambda$, pΩ, $\Xi\Xi$ and $\Omega\Omega$ are presented for central Au+Au collisions at $\sqrt{s_{NN}} = 11.5$ and 200 GeV.

The baryon–strangeness correlation coefficient C_{BS} is proposed as a diagnostic tool to understand the nature of matter formed in heavy ion collisions [32,33]. For QGP state the C_{BS} is expected to be unity, however a significant dependence of C_{BS} on hadronic environment is observed by V. Koch, A. Majumder and J. Randrup [32]. Measurement of C_{BS} in experiments is a technical challenge as one needs to measure baryon number and strangeness on event-by-event basis. Therefore the strangeness population factor S_3 was introduced by T.A. Armstrong et al. [34], which fairly depicts the local correlation between baryon number and strangeness [15]. Further we introduce S_2, which represents the local strangeness–strangeness correlations. Keeping in mind the technical challenges to measure C_{BS}, in this Letter, we concentrate on the strangeness

* Corresponding author.
E-mail addresses: neha@sinap.ac.cn, neau2802@gmail.com (N. Shah).

http://dx.doi.org/10.1016/j.physletb.2016.01.005

population factors S_3, S_2 for central Au+Au collisions at $\sqrt{s_{NN}}$ = 11.5 and 200 GeV.

2. Coalescence model

A naive coalescence model is used to study the production of multistrange hadrons, light nuclei and hypertriton in central Au+Au collisions at $\sqrt{s_{NN}} = 11.5$ and 200 GeV. It is assumed that the production of these particles occurs at the kinetic freeze-out stage. In this case the particle production probability is proportional to the primordial hadron density and can be described by following equation [35]:

$$E_c \frac{d^3N_c}{d^3p_c} = B(E_a \frac{d^3N_a}{d^3p_a})^n (E_b \frac{d^3N_b}{d^3p_b})^m, \quad (1)$$

where $E\frac{d^3N}{d^3p}$ are the invariant yield of particles (a, b and c) under consideration, p_c, p_a and p_b are their momenta, B is the coalescence parameter and $\vec{p}_c = n\vec{p}_a + m\vec{p}_b$. The phase space information from the hydrodynamic blast-wave model is used as an input to the equation (1) to calculate the invariant yields of $\Lambda\Lambda$, pΩ, $\Xi^0\Xi^-$, $\Omega\Omega$, light nuclei and hypertriton.

In hydrodynamic blast-wave model [36], the system is characterized by these parameters: the kinetic freeze-out temperature T_{kin}, the radial flow parameter ρ_0 and elliptic flow parameter ρ_2, the spatial anisotropy a, the average transverse radius R, and the particle emission duration τ_0. It is assumed that the fireball created in heavy ion collision is in local thermal equilibrium and moves outward with velocity u_μ. The phase–space emission points for hadrons are defined as a Wigner function:

$$S(x,p)d^4x = \frac{2s+1}{(2\pi)^3} m_t \cosh(y-\eta) exp(-\frac{p^\mu u_\mu}{T_k}) \times \Theta(1-\tilde{r}(r,\phi))H(\eta) \times \delta(\tau-\tau_0)d\tau\,\tau\,d\eta r dr d\phi, \quad (2)$$

where y is the rapidity, m_t is transverse mass, p^μ is four momentum, and (2s+1) is the degeneracy due to spin of hadrons. $\tilde{r}$ is given by

$$\tilde{r} = \sqrt{\frac{(x^1)^2}{{R_x}^2} + \frac{(x^2)^2}{{R_y}^2}},\ R_x = aR,\ R_y = \frac{R}{a}, \quad (3)$$

where (x^1, x^2) is the transverse position of the hadrons in coordinate space. Then we can define the azimuthally integrated p_T spectrum as

$$\frac{dN}{2\pi\, p_T dp_T} = \int S(x,p)d^4x. \quad (4)$$

Results obtained for the invariant yields of multistrange hadrons, nuclei and hypertriton using equations (1) and (4) are discussed in the next section.

3. Result and discussion

To study dibaryons, light nuclei and hypertriton production in the central Au+Au collisions at the RHIC energies 200 GeV and 11.5 GeV, we use following parameters derived from the STAR experiment at the RHIC as input to the hydrodynamic blast-wave model: kinetic freeze-out temperature = 89 (120) MeV, baryochemical potential = 21.9 (315) MeV, strangeness chemical potential = 6.5 (68) MeV and radial flow parameter ρ_0 = 0.91 (0.46) for the $\sqrt{s_{NN}} = 200$ (11.5) GeV [37]. The elliptic flow parameter $\rho_2 = 0$, spatial anisotropy a = 1, average transverse radius R = 10 fm and finite longitudinal proper time = 6.2 fm/c are set the same for both $\sqrt{s_{NN}} = 200$ GeV and 11.5 GeV [38–40]. Similar calculations were done by K.-J. Sun and L.-W. Chen in [20], where the freeze-out parameters are higher than the parameters used in our calculations. The proton spectra used from the PHENIX Collaboration to derive the freeze-out parameter in [20] are not corrected for the feed-down from Λ and Σ baryons. The coalescence of hadron occurs when $|\vec{r}_i - \vec{r}_j| < 2R_0$ and $|\vec{p}_i - \vec{p}_j| < 100$ MeV/c, where $(\vec{r}_i, \vec{p}_i)$ and $(\vec{r}_j, \vec{p}_j)$ are the phase–space position of the two constituent hadrons, and R_0 is the nuclear force radius. For deuteron and multistrange dibaryon $R_0 = 1.57$ fm is used and for the other nuclei $R_0 = 1.5$ fm is used.

The first two panels in Fig. 1 show differential yields of p, Λ, Ξ, Ω, $\Lambda\Lambda$, pΩ, $\Xi^0\Xi^-$ and $\Omega\Omega$ produced in central Au+Au collisions at $\sqrt{s_{NN}} = 200$ and 11.5 GeV respectively. Our calculation can reproduce the data for proton, Λ, Ξ and Ω from the STAR experiment at both energies [41–44]. The light (anti)nuclei and hypertriton spectra for $\sqrt{s_{NN}} = 11.5$ GeV are shown in third panel of Fig. 1. For $\sqrt{s_{NN}} = 200$ GeV the light (anti)nuclei spectra are taken from the article [19], where the same coalescence model was used. The p_T integrated yields for light nuclei and dibaryons in the central rapidity are given in Table 1. We observe that expected yields of all the particles at $\sqrt{s_{NN}} = 11.5$ GeV are significantly higher than $\sqrt{s_{NN}} = 200$ except for $\Omega\Omega$, maybe because of competition between strangeness production mechanisms at this energy.

Fig. 2 shows the rapidity distribution of p, Λ, Ξ, Ω, $\Lambda\Lambda$, pΩ, $\Xi^0\Xi^-$, $\Omega\Omega$, d, ^{3}He and hypertriton in central Au+Au collision at $\sqrt{s_{NN}} = 11.5$ GeV from the hydrodynamical blast-wave model plus a coalescence model. Since uniform rapidity distribution is used for $\sqrt{s_{NN}} = 200$ GeV, we have not shown those rapidity distributions here.

The p_T integrated yields dN/dy of multistrange hadrons as a function of strangeness $|S|$ for central Au+Au collisions at $\sqrt{s_{NN}} =$ 11.5 GeV (left) and 200 GeV (right) are shown in Fig. 3, where filled symbols are data from the STAR experiment [42–44] and different lines represent our calculations from the hydrodynamical blast-wave model plus a coalescence model. The $\Lambda\Lambda$ and $\Omega\Omega$ dibaryon production yields at top RHIC energy were estimated by the ExHIC Collaboration based on a realistic coalescence model and statistical model [27,28]. Those yields are compared with our calculations in the Fig. 3. We observe an exponential behavior of the invariant yield of multistrange hadrons similar to light nuclei [19]. The yield for baryon and dibaryon systems is fitted with function $N_S = N^i(\frac{1}{\lambda})^{|S|-1}$, where N^i is number of initial strange hadrons, λ is penalty factor and S is the strangeness. The penalty factor quantitatively tells us how hard it is to produce a hadron with strangeness $(|S|+1)$ compared to a hadron with strangeness $(|S|)$. We obtain $\lambda = 9.86$ for baryons and $\lambda = 4.62$ for dibaryon system from the model for central Au+Au collisions at $\sqrt{s_{NN}} = 11.5$ GeV. Similarly we obtain $\lambda = 6.46$ for baryons and $\lambda = 4.21$ for dibaryon system from the model for central Au+Au collisions at $\sqrt{s_{NN}} =$ 200 GeV. By fitting the data from the STAR experiment for baryons, we get $\lambda = 12.92 \pm 1.04$ (5.71 ± 0.34) for the central Au+Au collisions at $\sqrt{s_{NN}} = 11.5$ (200) GeV.

Fig. 4 shows the production rate of nuclei as a function of baryon number for the central Au+Au collisions at $\sqrt{s_{NN}} =$ 11.5 GeV and 200 GeV, where solid points are our calculations using the coalescence model and open symbols are data from the STAR experiment [10]. At $\sqrt{s_{NN}} = 200$ GeV, our results are consistent with the STAR measurement within the uncertainties. The production rates exhibit a decreasing exponential behavior with the increase in baryon number. Further we obtain the reduction factor by fitting the data with exponential function e^{-rB}. Obtained fit values for reduction factor are 1.2×10^3 (1.5×10^3) and 0.33×10^3 (1.95×10^4) for adding one more nucleon (antinucleon)

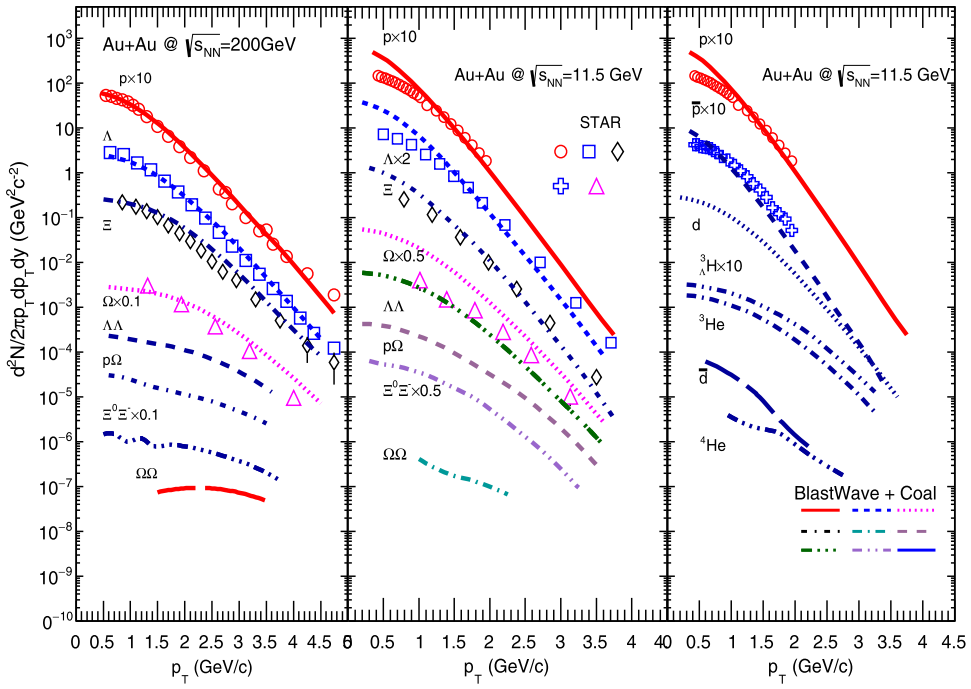

Fig. 1. (Color online.) Differential invariant yields versus p_T distribution for p, Λ, Ξ, Ω, $\Lambda\Lambda$, $p\Omega$, $\Xi^0\Xi^-$, $\Omega\Omega$, light (anti)nuclei and hypertriton produced in central Au+Au collisions at $\sqrt{s_{NN}} = 11.5$ and 200 GeV. The filled symbols are data from STAR experiment [41–44] and different lines represent our calculations from the hydrodynamical blast-wave model plus a coalescence model.

Table 1
p_T integrated yields of light nuclei, hypertriton and dibaryons in Au+Au collisions.

$\sqrt{s_{NN}}$ (GeV)	$dN_{^3\mathrm{He}}/dy$	$dN_{^3_\Lambda\mathrm{H}}/dy$	$dN_{^4\mathrm{He}}/dy$	$dN_{\Lambda\Lambda}/dy$	$dN_{p\Omega}/dy$	$dN_{\Xi^0\Xi^-}/dy$	$dN_{\Omega\Omega}/dy$
11.5	1.06×10^{-2}	2.04×10^{-3}	3.63×10^{-5}	2.46×10^{-2}	2.12×10^{-3}	6.68×10^{-4}	1.63×10^{-6}
200	1.65×10^{-4}	1.05×10^{-4}	3.30×10^{-7}	7.24×10^{-3}	4.24×10^{-4}	2.75×10^{-4}	3.25×10^{-6}

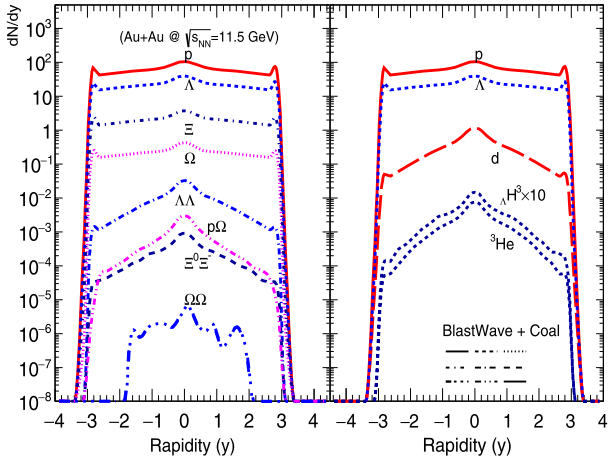

Fig. 2. (Color online.) The rapidity distribution of multistrange hadrons, light nuclei and hypertriton in central Au+Au collisions at $\sqrt{s_{NN}} = 11.5$ GeV.

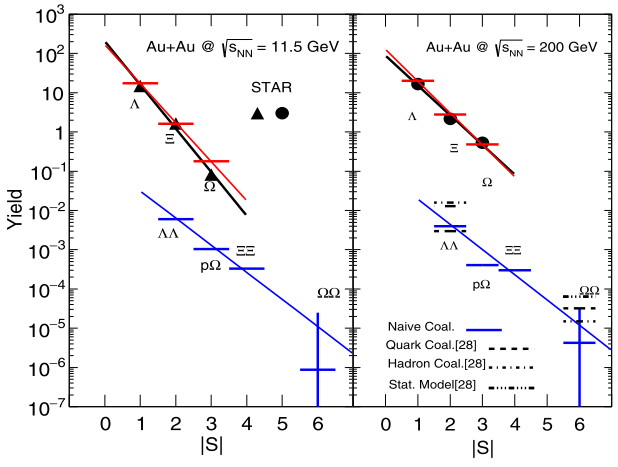

Fig. 3. (Color online.) p_T integrated yields dN/dy of multistrange hadrons as a function of strangeness $|S|$ for central Au+Au collisions at $\sqrt{s_{NN}} = 11.5$ GeV (left) and 200 GeV (right). The filled symbols are data from the STAR experiment [42–44], the solid lines represent our calculations from the hydrodynamical blast-wave model plus a coalescence model and the dashed lines for the $\Lambda\Lambda$ and $\Omega\Omega$ dibaryons are from Ref. [28].

to the system for $\sqrt{s_{NN}} = 200$ and 11.5 GeV respectively. The reduction factor obtained from our calculation at $\sqrt{s_{NN}} = 200$ GeV is comparable with $1.1^{+0.3}_{-0.2} \times 10^3$ ($1.6^{+1.0}_{-0.6} \times 10^3$) obtained by the STAR experiment [10]. The production rates for nuclei at $\sqrt{s_{NN}} = 11.5$ GeV are significantly higher than $\sqrt{s_{NN}} = 200$ GeV where the rates decrease sharply for antinuclei at the same energy compared to $\sqrt{s_{NN}} = 200$ GeV. The difference in reduction factors between matter and antimatter shows a significant energy (or temperature) dependence, which illustrates an increasing matter–antimatter asymmetry of the yields at lower energies (temperatures). If we make a rough extension to current Universe at room temperature, we can hardly observe the antimatter existence,

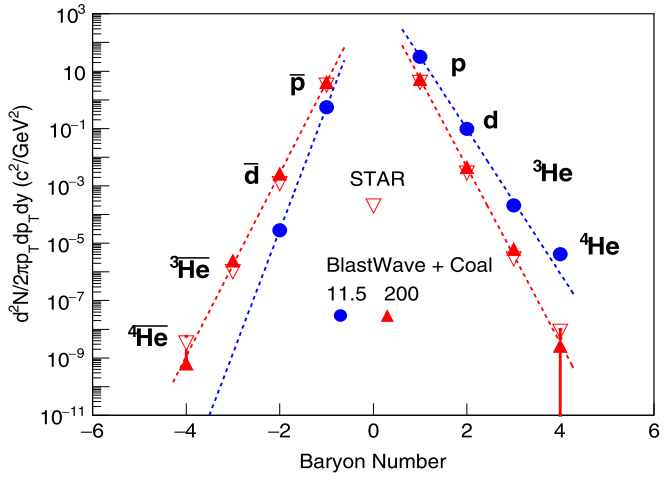

Fig. 4. (Color online.) Invariant yield of nuclei in the average transverse momentum region ($p_T/|B| = 0.875$ GeV/c) as a function of baryon number B for central Au+Au collisions at $\sqrt{s_{NN}} = 11.5$ GeV and 200 GeV. Open symbols are data from STAR experiment [10], solid points are our calculations from coalescence model and different lines represent fit to the coalescence model and data from STAR experiment [10].

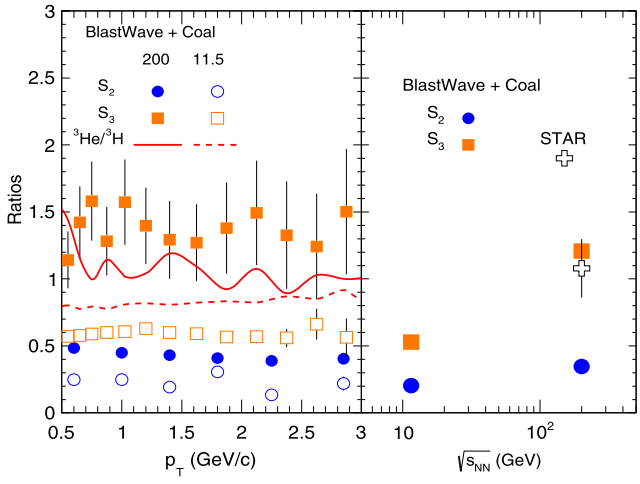

Fig. 5. (Color online.) On left ratios S_2, S_3 and $\frac{^3\text{He}}{^3\text{H}}$ are plotted as a function of transverse momentum (p_T) for central Au+Au collisions at $\sqrt{s_{NN}} = 11.5$ GeV and 200 GeV. On right ratios S_2 and S_3 are plotted as a function of beam energy $\sqrt{s_{NN}}$, where open cross is data from STAR experiment [9].

which is consistent with the current observation of the cosmic rays from which neither antideutron nor antihelium is observed [45,46].

The strangeness population factor $S_3 = {}^3_\Lambda\text{H}/({}^3\text{He} \times \frac{\Lambda}{p})$ contains the local baryon–strangeness correlation in the numerator and the baryon–baryon correlation in the denominator [15,35]. Therefore S_3 is quantitatively a good representation of χ_{11}^{BS}/χ_2^B, where χ is the second derivative of the free energy with respect to the chemical potential, from lattice QCD [47]. The ratio S_3 as a function transverse momentum is shown in Fig. 5(left). Similarly we define $S_2 = \Lambda\Lambda/(d \times (\Lambda/p)^2)$ for strangeness $= -2$ dibaryon which contains the local strangeness–strangeness correlation in the numerator and the baryon–baryon correlation in the denominator. An increase in ratios S_2 and S_3 is observed for Au+Au collisions at $\sqrt{s_{NN}} = 200$ GeV compared to $\sqrt{s_{NN}} = 11.5$ GeV as shown in Fig. 5(right). The ratios $\frac{^3\text{He}}{^3\text{H}}$ for $\sqrt{s_{NN}} = 11.5$ GeV and 200 GeV are also shown in Fig. 5(left). We observe that the ratio $\frac{^3\text{He}}{^3\text{H}}$ at $\sqrt{s_{NN}} = 11.5$ GeV is lower than unity, where the isospin effects become important compared to $\sqrt{s_{NN}} = 200$ GeV.

4. Conclusion

We presented an interesting calculation for the production of dibaryons, light (anti)nuclei and hypertriton, based on a naive coalescence model for Au+Au collisions at $\sqrt{s_{NN}} = 11.5$ and 200 GeV. The exponential behavior of the invariant yields versus strangeness is studied for the multistrange hadrons and penalty factor for the baryon and dibaryon is derived. The ratios S_2 and S_3 are discussed for Au+Au collisions at $\sqrt{s_{NN}} = 11.5$ and 200 GeV. We observe an increase in S_2 and S_3 at $\sqrt{s_{NN}} = 200$ GeV compared to $\sqrt{s_{NN}} = 11.5$ GeV. Furthermore our study indicates that the suppression factor for nuclei production at $\sqrt{s_{NN}} = 11.5$ GeV is roughly four times smaller than suppression factor at $\sqrt{s_{NN}} = 200$ GeV; leading to higher probability for observation of light nuclei candidates at lower energy. Our calculation will provide the motivation to carry out measurement of S_3, light nuclei and dibaryons during the phase-II of beam energy scan program at STAR experiment at RHIC [48].

Acknowledgements

This work is supported in part by the Major State Basic Research Development Program in China under Contract No. 2014CB845400, the National Natural Science Foundation of China under contract Nos. 11421505, 11520101004, 11275250, 11322547, U1232206. Author N. Shah is supported by Chinese Academy of Sciences (CAS) President's International Fellowship Initiative No. 2015PM029.

References

[1] I. Aresene, et al., BRAHMS Collaboration, Nucl. Phys. A 757 (2005) 1.
[2] B.B. Back, et al., PHOBOS Collaboration, Nucl. Phys. A 757 (2005) 28.
[3] J. Adams, et al., STAR Collaboration, Nucl. Phys. A 757 (2005) 102.
[4] K. Adcox, et al., PHINEX Collaboration, Nucl. Phys. A 757 (2005) 184.
[5] Y.G. Ma, J.H. Chen, L. Xue, Front. Phys. 7 (2012) 637.
[6] Y.G. Ma, J.H. Chen, L. Xue, A. Tang, Z. Xu, Nucl. Phys. News 23 (2013) 10.
[7] M. Hori, J. Walz, Prog. Part. Nucl. Phys. 72 (2013) 206.
[8] C.M. Ko, et al., Nucl. Sc. Techniques 24 (2013) 050525.
[9] B.I. Abelev, et al., STAR Collaboration, Science 328 (2010) 58; J.H. Chen, Nucl. Phys. A 835 (2010) 117.
[10] H. Agakishiev, et al., STAR Collaboration, Nature 473 (2011) 353; L. Xue, J. Phys. G 38 (2011) 124072.
[11] ALICE Collaboration, arXiv:1506.08453.
[12] L. Adamczyk, et al., STAR Collaboration, Nature 527 (2015) 345.
[13] A. Andronic, P. Braun-Munzinger, J. Stachel, H. Stöcker, Phys. Lett. B 697 (2011) 203.
[14] J. Cleymans, S. Kabana, I. Kraus, H. Oeschler, K. Redlich, N. Sharma, Phys. Rev. C 84 (2011) 054916.
[15] S. Zhang, J.H. Chen, H. Crawford, D. Keane, Y.G. Ma, Z.B. Xu, Phys. Lett. B 684 (2010) 224.
[16] G. Chen, H. Chen, J. Wu, D.S. Li, M.J. Wang, Phys. Rev. C 88 (2013) 034908.
[17] A.S. Botvina, J. Steinheimer, E. Bratkovskaya, M. Bleicher, J. Pochodzalla, Phys. Lett. B 747 (2013) 7.
[18] L. Zhu, C.M. Ko, X. Yin, arXiv:1510.03568.
[19] L. Xue, Y.G. Ma, J.H. Chen, S. Zhang, Phys. Rev. C 85 (2012) 064912; L. Xue, Y.G. Ma, J.H. Chen, S. Zhang, Phys. Rev. C 92 (2015) 059901 (Erratum).
[20] K.J. Sun, L.W. Chen, Phys. Lett. B 751 (2015) 272.
[21] R. Jaffe, Phys. Rev. Lett. 38 (1977) 195.
[22] T. Golman, K. Maltman, F. Wang, Phys. Rev. Lett. 59 (1987) 627.
[23] G.A. Miller, Chin. J. Phys. 51 (2013) 466.
[24] Z.Y. Zhang, Y.W. Yu, C.R. Ching, T.H. Ho, Z.D. Lu, Phys. Rev. C 61 (2000) 065204.
[25] L. Adamczyk, et al., STAR Collaboration, Phys. Rev. Lett. 115 (2015) 022301; N. Shah, STAR Collaboration, Nucl. Phys. A 914 (2013) 410.
[26] ALICE Collaboration, arXiv:1506.07499 [nucl-ex].
[27] S. Cho, et al., ExHIC Collaboration, Phys. Rev. Lett. 106 (2011) 212001.
[28] S. Cho, et al., ExHIC Collaboration, Phys. Rev. C 84 (2011) 064910.
[29] S.R. Beane, et al., NPLQCD Collaboration, Phys. Rev. Lett. 106 (2011) 162001.
[30] T. Inoue, et al., HAL QCD Collaboration, Phys. Rev. Lett. 106 (2011) 162002.

[31] P.E. Shanahan, A.W. Thomas, R.D. Young, Phys. Rev. Lett. 107 (2011) 092004.
[32] V. Koch, A. Majumder, J. Randrup, Phys. Rev. Lett. 95 (2005) 182301.
[33] S. Haussler, S. Scherer, M. Bleicher, Phys. Lett. B 660 (2008) 197.
[34] T.A. Armstrong, et al., E864 Collaboration, Phys. Rev. C 70 (2004) 024902.
[35] H. Sato, K. Yazaki, Phys. Lett. B 98 (1981) 153.
[36] F. Retière, M.A. Lisa, Phys. Rev. C 70 (2004) 044907.
[37] L. Kumar, STAR Collaboration, Nucl. Phys. A 931 (2014) 1114.
[38] K. Geiger, Phys. Rep. 258 (1995) 237.
[39] J.W. Harris, B. Müller, Annu. Rev. Nucl. Part. Sci. 46 (1996) 71.
[40] B. Müller, Nucl. Phys. A 630 (1998) 461c.
[41] B.I. Abelev, et al., STAR Collaboration, Phys. Lett. B 655 (2007) 104.
[42] G. Agakishiev, et al., STAR Collaboration, Phys. Rev. Lett.108 (2012) 072301.
[43] J. Adams, et al., STAR Collaboration, Phys. Rev. Lett. 98 (2007) 062301.
[44] X. Zhu, STAR Collaboration, Acta Phys. Pol. B, Proc. Suppl. 5 (2012) 213;
F. Zhao, STAR Collaboration, Thesis, University of California, Los Angeles, 2014.
[45] H. Fuke, et al., Phys. Rev. Lett. 95 (2005) 081101.
[46] K. Abe, et al., Phys. Rev. Lett. 108 (2012) 131301.
[47] M. Cheng, et al., Phys. Rev. D 79 (2009) 074505.
[48] Studying the phase diagram of QCD matter at RHIC, STAR Collaboration, SN0598, 2014.